

One-way total reflection with one-dimensional magneto-optical photonic crystals

Zongfu Yu^{a)} and Zheng Wang

Department of Applied Physics, Stanford University, Stanford, California 94305

Shanhui Fan

Ginzton Laboratory, Department of Electrical Engineering, Stanford University, Stanford, California 94305

(Received 1 October 2006; accepted 19 February 2007; published online 23 March 2007)

The authors show that one-dimensional magneto-optical photonic crystals can achieve one-way total reflection. The unit cell of the crystal, which consists of two bismuth iron garnet layers with opposite magnetization and one SiO₂ layer, is designed to simultaneously break time-reversal, spatial inversion, and mirror symmetries. Such crystals are important for creating compact broadband optical isolators. © 2007 American Institute of Physics. [DOI: 10.1063/1.2716359]

Magneto-optical photonic crystals are of interest because they provide mechanisms to miniaturize nonreciprocal components and to strongly enhance magneto-optical effects. Some notable recent developments include the observation of cavity-enhanced Faraday rotation¹⁻⁴ in one-dimensional (1D) magneto-optical photonic crystal, as well as theoretical proposals regarding nonreciprocal superprisms⁵ and ultra-compact isolators.^{6,7} In all of these works, a wave and its time-reversed counterpart either both fall within the band or within the band gap. Since the practical goal of these devices is to create large contrasts between such two waves, it should be of interest to design structures in which only one of the waves falls within the gap, and thus the structures exhibit one-way total reflection. In this letter, we report the design of photonic crystals that exhibit one-way total reflection at the interface between the crystals and homogenous media. Such design provides a mechanism to construct optical isolators with the Voigt geometry.^{8,9}

Consider an interface normal to the direction of periodicity of a 1D crystal, between air and the crystal (Fig. 1). For an incident light from air, the wave vector component parallel to the interface, defined as k_x , is conserved. In order to create a one-way total reflector at a given frequency ω , the crystal should support a propagation mode at $k_x = n_0(\omega/c)\sin\theta$, but not at $k_x = -n_0(\omega/c)\sin\theta$, where $n_0 = 1$ is the refractive index of air and θ is the angle of incidence. A necessary condition to do so is to break the inversion symmetry of band structure in \mathbf{k} space, i.e.,

$$\omega(\mathbf{k}) \neq \omega(-\mathbf{k}), \quad (1)$$

which requires simultaneous breaking of spatial inversion and time-reversal symmetries.^{10,11} However, Eq. (1) is not sufficient for our purpose here. For example, for the one-dimensional crystal as shown in Fig. 1, with the direction of periodicity along the y direction, at normal incidence due to the Bloch theorem we have $\omega(k_x=0, k_y=\pi/a) = \omega(k_x=0, k_y=-\pi/a)$, where a is the periodicity of the crystal. Therefore, at $k_x=0$, the forward and backward waves inside the crystal always cover the same frequency ranges and thus one-way total reflection cannot happen, in spite of the fact that coun-

terpropagating waves with the same frequency may correspond to k_y 's of different magnitudes.

In order to realize a one-way total reflector, we therefore need to create a crystal where the band edges are not fully aligned for allowed modes at k_x and $-k_x$. Thus, in addition to time-reversal symmetry, one needs to further break all symmetry operations that map $x \rightarrow -x$. These include, in addition to the spatial inversion operation in two dimensions σ , the mirror reflection operation π_x with its mirror-plane normal to the x direction.

We accomplish the required symmetry breaking with the use of a gyrotropic material, Bismuth iron garnet (BIG), in 1D photonic crystals. The optical property of BIG is characterized by a dielectric tensor of the following form

$$\vec{\epsilon} = \begin{pmatrix} \epsilon_{\perp} & -i\epsilon_a & 0 \\ i\epsilon_a & \epsilon_{\perp} & 0 \\ 0 & 0 & \epsilon_{\parallel} \end{pmatrix} = \vec{\epsilon}_d + i\epsilon_a \hat{z} \times \vec{I}, \quad (2)$$

when the magnetization is along the z direction. $\vec{\epsilon}_d$ is the diagonal part. For BIG, $\epsilon_{\perp} = 6.25$ and $\epsilon_a = 0.06$.^{12,13} For concreteness, we consider the Voigt geometry, where light propagates in the plane perpendicular to \hat{z} . In this geometry, TE and TM modes (with H or E fields polarized along the z direction, respectively) are completely decoupled.¹⁴ The TM modes are related only to the tensor element ϵ_{\parallel} and still possess time-reversal symmetry. Thus, in the following discussions we focus only on the TE modes.

With respect to coordinate transformations, the dielectric tensor $\vec{\epsilon}(\mathbf{r})$ in Eq. (2) transforms as

$$\begin{aligned} \sigma^{-1} \vec{\epsilon} \sigma &= \vec{\epsilon}, \\ \pi_x^{-1} \vec{\epsilon} \pi_x &= \vec{\epsilon}_d - i\epsilon_a \hat{z} \times \vec{I}. \end{aligned} \quad (3)$$

The dielectric tensor itself is invariant under spatial inversion operation σ , while the mirror operation π_x effectively flips the magnetization direction. In order to break spatial inversion symmetry, the simplest structure consists of three layers in a primitive cell (Fig. 1). Two of the layers are gyrotropic with opposite magnetization and the third layer can be an isotropic reciprocal material. Such a structure also breaks mirror symmetry along the x direction. In contrast, any 1D crystal structure with two layers per unit cell always maintains spatial inversion symmetry and is therefore not useful

^{a)}Electronic mail: zfyu@stanford.edu

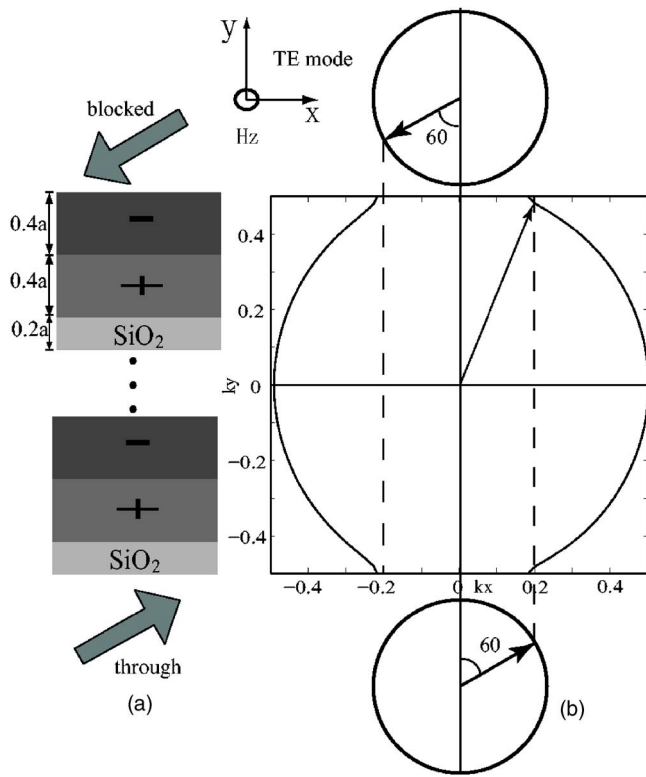


FIG. 1. (Color online) (a) Schematics of the finite-length 1D magneto-optical PC functioning as an optical isolator, where the arrows represent light incident from air. Each primitive cell consists of two high-index BIG layers, with opposite magnetic directions along z directions, and a low-index SiO_2 layer. The lattice constant is a . (b) Constant-frequency contours of TE modes at $\omega=0.226 \ 2\pi c/a$. The wave vectors of the incident and the refracted waves are marked with the arrows.

for our purpose. The use of the reciprocal dielectric material (such as SiO_2 glass, in which the Verdet constant is orders of magnitude smaller than that of BIG and is therefore negligible) further provides good index contrast with BIG to create the band gap.

The strength of the nonreciprocal effects depends on the thickness of the layers. With the magnitude of magnetization in the two gyrotropic layers being equal, an equal thickness gives the maximal nonreciprocal effects.⁷ For the structure shown in Fig. 1, the magnetic material needs to be thick enough to create nonreciprocal effects. The SiO_2 layer, on the other hand, also needs to be thick enough to create band gaps. As a compromise between these two competing requirements, we use a thickness of $0.2a$ for SiO_2 and $0.4a$ for the two gyrotropic layers [Fig. 1(a)].

The one-way total reflection at the interface between air and an optimized 1D photonic crystal (PC) is illustrated in Fig. 1(b). To highlight the effect of asymmetric band gaps, we have used $\epsilon_a=0.6$, which is ten times greater than the realistic material constant. The calculated constant-frequency contour shows clear asymmetry with respect to the $k_x=0$ axis. A plane wave at $\omega=0.226(2\pi c/a)$, incident from above the crystal with 60° incident angle, falls within the band gap and becomes completely reflected. In contrast, a time-reversed wave, incident from below the crystal, falls within the propagating band and passes through the crystal. Such a structure thus demonstrates one-way total reflection.

To further visualize the operating angular and frequency range of such “one-way” total reflection, we plot in Fig. 2 the frequencies of modes in the first two bands at the wave vec-

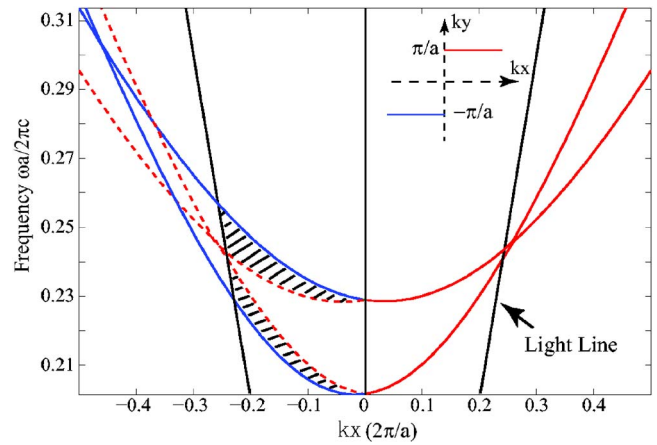


FIG. 2. (Color online) Frequencies of the modes in the structure shown in Fig. 1, for the first two bands at the wave vectors $(k_x, k_y = \pm \pi/a)$. The locations of the wave vectors are depicted in the inset. The red and blue solid curves correspond to wave vectors at $(k_x, k_y = +\pi/a)$ and $(-k_x, k_y = -\pi/a)$, respectively. The dashed red curves are the mirror reflection of the red solid curves. The shaded regions indicate the operation range of one-way total reflection.

tors $(k_x, k_y = \pm \pi/a)$, since in this structure, the edges of the first band gap are located at these wave vectors. As can be seen from Fig. 2, the frequencies of the gap edges differ for modes at $\pm k_x$. At a given angle of incidence, the operating frequency range can be derived from this difference. Also, at a given frequency, the difference in the gap region above the light line ($\omega = ck_x$) provides the operating angular range. Therefore, lowering the position of the light line, for example, by using a high-index medium outside the crystal, provides greater angular range of operation.

From the projected band-edge diagram, one can also estimate the number of periods needed to achieve significant contrast between the two counterpropagating waves. In the crystals, the decay length L of a mode lying in the band gap is estimated by its distance Δk to the closest band gap edge in \mathbf{k} space: $L \sim 1/\Delta k$. Therefore, for the device to operate, the length of the crystal in wave propagating direction has to be greater than $1/\Delta k$. For the calculated structure in Fig. 2 with $\epsilon_a=0.6$, the largest possible Δk in the operating region is about $0.04(2\pi/a)$. With $\epsilon_a=0.06$ in BIG, Δk is estimated to be $0.004(2\pi/a)$, since Δk is proportional to the strength of magneto-optical effects. This translates to $L \approx 40a$.

As a validation of the photonic crystal design based on band structure analysis, here we directly determine the response of a finite structure using transfer matrix formalism.¹⁵ In this calculation we assume a realistic BIG material constant ($\epsilon_a=0.06$). Figure 3 shows the transmission spectra of a finite-length crystal with a thickness of $100a$. Counter-propagating plane waves are incident from air upon either end of the crystal. Full transmission is obtained along one direction, while complete reflection is obtained in the opposite direction, clearly demonstrating the desired nonreciprocal effects. The effect of one-way reflection is visualized in Figs. 3(b) and 3(c), which shows the field pattern at $\omega=0.2259(2\pi c/a)$. The transmission contrast ratio between the two directions at this frequency is 94 dB.

The operation range of frequency is ideally set by the difference between the two band edges as shifted due to magneto-optical effects. However, significant Fabry-Pérot oscillation is observed in the spectrum [Fig. 3(a)], which

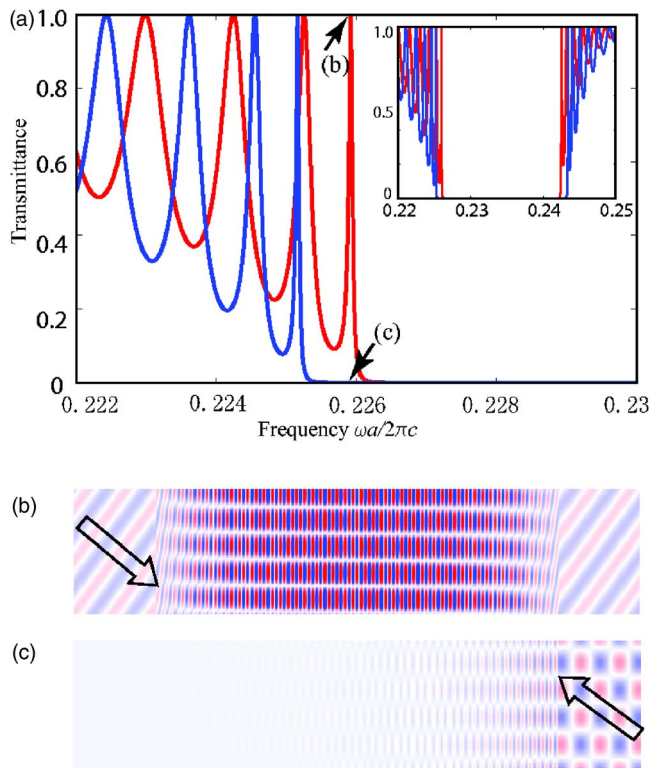


FIG. 3. (Color online) (a) Transmittance spectra of front- (the red trace) and back-illuminated (the blue trace) photonic crystal isolators with a thickness of $100a$. The calculations are for $k_x=0.4\pi/a$ (red) and $k_x=-0.4\pi/a$ (blue). The inset shows the spectrum for a wider frequency range. [(b) and (c)] Steady state magnetic field distribution for $\omega=0.226\ 2\pi c/a$ under front illumination (b) and back illumination (c).

reduces the frequency range for practical operations. To suppress the oscillation in the transmission spectra, we introduce a transition region close to the crystal-air interface.¹⁶ In this region, as one approaches the crystal-air interface, the thickness of the gyrotropic material layers in each unit cell is gradually reduced from $0.8a$ to $0a$ with a parabolic profile, while the SiO_2 layer thickness increases to maintain the same cell size. We calculate the transmittance for such a reflector consisting of $50a$ of periodic structure, sandwiched by transition regions with thickness of $40a$ on each side. The Fabry-Pérot oscillations are strongly suppressed, resulting in a greatly increased operation bandwidth (Fig. 4).

Compared with one-dimensional photonic crystal structures with enhanced Faraday rotation, here no polarizer is needed to create a nonreciprocal effect in the amplitude response for linearly polarized light. The frequency bandwidth for a contrast ratio above 30 dB in the structure of Fig. 4 is 2.5 THz at 633 nm wavelength. Thus the operation of this structure is relatively broadband. The lattice constant a is about $0.14\ \mu\text{m}$. A 50-lattice device including the transition layers has a length of only $18.2\ \mu\text{m}$ in the light propagation direction. The dimensions of the magnetic domain used here are, in fact, consistent with experimental structures.^{17–19} Also, one may be able to make the structure magnetically stable by placing a thin nonmagnetic layer in between the magnetic domain layers that have opposite magnetization directions. This thin nonmagnetic layer serves to suppress the ferromagnetic coupling between nearest neighbor spins, and therefore only needs to be several nanometer thick, which would not affect the optical properties we discuss here. The

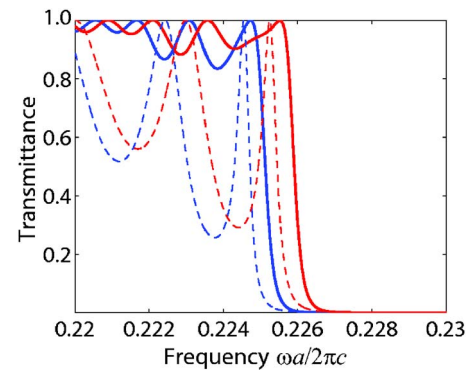


FIG. 4. (Color online) Solid lines are transmittance spectra of a crystal with a thickness of $50a$, and with transition layers close to the crystal-air interface for front (red curve) and back (blue curve) illuminations. The angle of incidence is 62.3° . The dashed curves are for a crystal with a thickness of $50a$ without the transition layers.

magnetization of each layer may then be locked in by the kind of flux closure arrangement similar to Refs. 20 and 21. In addition, it is likely that the idea proposed here can be implemented in structures using layers with vertical magnetizations, as seen in Ref. 22.

The authors acknowledge S. X. Wang for helpful discussions. This work was supported in part by the National Science Foundation Grant No. ECS-0622212, and a Packard Fellowship.

- ¹R. Wolfe, R. A. Lieberman, V. J. Fratello, R. E. Scotti, and N. Kopylov, *Appl. Phys. Lett.* **56**, 426 (1990).
- ²M. Levy, I. Ilic, R. Scarmozzino, R. M. Osgood, Jr., R. Wolfe, C. J. Gutierrez, and G. A. Prinz, *IEEE Photonics Technol. Lett.* **5**, 198 (1993).
- ³M. Inoue, K. Arai, T. Fujii, and M. Abe, *J. Appl. Phys.* **83**, 6768 (1998).
- ⁴M. J. Steel, M. Levy, and R. M. Osgood, *IEEE Photonics Technol. Lett.* **12**, 1171 (2000).
- ⁵I. Bita and E. L. Thomas, *J. Opt. Soc. Am. B* **22**, 1199 (2005).
- ⁶Z. Wang and S. Fan, *Opt. Lett.* **30**, 1989 (2005).
- ⁷Z. Wang and S. Fan, *Appl. Phys. B: Lasers Opt.* **81**, 369 (2005).
- ⁸T. Mizumoto, S. Mashimo, T. Ida, and Y. Naito, *IEEE Trans. Magn.* **29**, 3417 (1993).
- ⁹J. Fujita, M. Levy, R. M. Osgood, L. Wilkens, and H. Dötsch, *Appl. Phys. Lett.* **76**, 2158 (2000).
- ¹⁰A. Figotin and I. Vitebsky, *Phys. Rev. E* **63**, 066609 (2001).
- ¹¹I. Vitebsky, J. Edelkind, E. Bogachek, and Uzi Landman, *Phys. Rev. B* **55**, 12566 (1997).
- ¹²T. Tepper and C. A. Ross, *J. Cryst. Growth* **255**, 324 (2003).
- ¹³N. Adachi, V. P. Denysenkov, S. I. Khartsev, A. M. Grishin, and T. Okuda, *J. Appl. Phys.* **88**, 2734 (2000).
- ¹⁴J. D. Joannopoulos, R. D. Meade, and J. N. Winn, *Photonic Crystals: Molding the Flow of Light* (Princeton University Press, Princeton, 1995), p. 22.
- ¹⁵B. E. A. Saleh and M. C. Teich, *Fundamentals of Photonics* (Wiley, New York, 1991), p. 193.
- ¹⁶Y. H. Ye, J. Ding, D. Y. Jeong, I. C. Khoo, and Q. M. Zhang, *Phys. Rev. E* **69**, 056604 (2004).
- ¹⁷A. Sandhu, H. Masuda, A. Oral, and S. J. Bending, *Jpn. J. Appl. Phys., Part 2* **40**, L524 (2001).
- ¹⁸I. L. Lyubchanskii, N. N. Dadoenkova, M. I. Lyubchanskii, E. A. Shapovalov, and T. H. Rasing, *J. Phys. D* **36**, R277 (2003).
- ¹⁹N. Spaldin, *Magnetic Materials: Fundamentals and Device Applications* (Cambridge University Press, Cambridge, 2003), p. 73.
- ²⁰J. C. Slonczewski, *IEEE Trans. Magn.* **26**, 1322 (1990).
- ²¹D. A. Herman, Jr., B. E. Argyle, P. L. Trouilloud, B. Petek, L. T. Romankiw, P. C. Andricacos, S. Krongelb, D. L. Rath, D. F. Canaperi, and M. L. Komsa, *J. Appl. Phys.* **63**, 4033 (1988).
- ²²V. J. Fratello and R. Wolfe, *Epitaxial Garnet Films for Nonreciprocal Magneto-Optic Devices*, Handbook of Thin Film Devices Vol. 4, edited by H. Francombe (Academic, New York, 2000), pp. 122–124.